Current Research in Food Science 7 (2023) 100547

Contents lists available at ScienceDirect

Current Research in Food Science

journal homepage: www.sciencedirect.com/journal/current-research-in-food-science

Tuna trimmings *(Thunnas albacares)* hydrolysate alleviates immune stress and intestinal mucosal injury during chemotherapy on mice and identification of potentially active peptides

Xiangtan Zhao [a,b,d], Bingna Cai [a,c], Hua Chen [a,c], Peng Wan [a,c], Deke Chen [a,c], Ziqing Ye [a,b,d], Ailing Duan [a,b,d], Xin Chen [e], Huili Sun [a], Jianyu Pan [a,c,d,*]

[a] *Key Laboratory of Tropical Marine Bio-Resources and Ecology, Guangdong Key Laboratory of Marine Materia Medica, South China Sea Institute of Oceanology, Chinese Academy of Sciences, 164 West Xingang Road, Guangzhou, 510301, China*
[b] *University of Chinese Academy of Sciences, Beijing, 100049, China*
[c] *Southern Marine Science and Engineering Guangdong Laboratory(Guangzhou), Guangzhou, 511458, China*
[d] *Innovation Academy of South China Sea Ecology and Environmental Engineering (ISEE), Chinese Academy of Sciences, China*
[e] *Foshan University, School of Environment and Chemical Engineering, Foshan, 528000, China*

ARTICLE INFO

Handling Editor: Dr. Yeonhwa Park

Keywords:
Tuna trimmings
Protein hydrolysate
Chemotherapy
Anti-tumor
Immune regulation
Intestinal mucosal damage

ABSTRACT

In this study, Tuna trimmings (*Thunnas albacares*) protein hydrolysate (TPA) was produced by alcalase. The anti-tumor synergistic effect and intestinal mucosa protective effect of TPA on S180 tumor-bearing mice treated with 5-fluorouracil (5-FU) chemotherapy were investigated. The results showed that TPA can enhance the anti-tumor effect of 5-FU chemotherapy, as evident by a significant reduction in tumor volume observed in the medium and high dose TPA+5-FU groups compared to the 5-FU group ($p < 0.001$). Moreover, TPA significantly elevated the content of total protein and albumin in all TPA dose groups ($p < 0.01$, $p < 0.001$), indicating its ability to regulate the nutritional status of the mice. Furthermore, histopathological studies revealed a significant increase in the height of small intestinal villi, crypt depth, mucosal thickness, and villi area in the TPA+5-FU groups compared to the 5-FU group ($p < 0.05$), suggesting that TPA has a protective effect on the intestinal mucosa. Amino acid analysis revealed that TPA had a total amino acid content of 66.30 g/100 g, with essential amino acids accounting for 30.36 g/100 g. Peptide molecular weight distribution analysis of TPA indicated that peptides ranging from 0.25 to 1 kDa constituted 64.54%. LC-MS/MS analysis identified 109 peptide sequences, which were predicted to possess anti-cancer and anti-inflammatory activities through database prediction. Therefore, TPA has the potential to enhance the antitumor effects of 5-FU, mitigate immune depression and intestinal mucosal damage induced by 5-FU. Thus, TPA could be serve as an adjuvant nutritional support for malnourished patients undergoing chemotherapy.

1. Introduction

Proteins serve as the foundation for sustaining the body's vital functions (Chakniramol et al., 2022). Dietary protein provides amino acids that support the growth and maintenance of cells and tissues. Moreover, food proteins release bioactive peptides (BP) that perform various biological and functional roles. These BP are composed of specific amino acids that can positively affect the body by regulating physiological responses (Daroit and Brandelli, 2021). However, these short amino acid sequences do not exert their activity in their original protein state and require proteolysis (*in vivo* digestion, *in vitro* enzymatic hydrolysis or bacterial fermentation) to release their biological potential (Chakrabarti et al., 2014). As research progresses, there has been a significant increase in isolating, purifying, and characterizing BP derived from marine sources. Additionally, the exploration of marine processing by-products and underutilized marine organisms, particularly fish, have been identified as promising sources of BP (Chakniramol et al., 2022).

Fish protein hydrolysates and peptides produced by different hydrolysis methods have been reported showing significant antioxidant (Zhao et al., 2019; Cai et al., 2022), anticancer (anti-proliferative effect) (Wang

* Corresponding author. Key Laboratory of Tropical Marine Bio-Resources and Ecology, Guangdong Key Laboratory of Marine Materia Medica, South China Sea Institute of Oceanology, Chinese Academy of Sciences, 164 West Xingang Road, Guangzhou, 510301, China.
E-mail address: jypan@scsio.ac.cn (J. Pan).

https://doi.org/10.1016/j.crfs.2023.100547
Received 25 April 2023; Received in revised form 3 July 2023; Accepted 3 July 2023
Available online 6 July 2023

et al., 2021; Yuan et al., 2021), antibacterial (Houyvet et al., 2018; Cipolari et al., 2020) and immunomodulatory activities (Kundam et al., 2018). Enzymatic hydrolysis is an effective method for extracting BP, which is more economical, easier to control, and relatively safer than other methods for recovering physiological and nutritional peptides from fish by-products (Idowu and Benjakul, 2019; Sridhar et al., 2021). The use of hydrolases produces fish protein hydrolysates (FPHs) that are rich in nutrition and BP and amino acids (Sinthusamran et al., 2020; Idowu et al., 2019). In a study, rainbow trout skin (*Oncorhynchus mykiss*) was hydrolyzed using alcalase and flavourzyme to yielded rainbow trout peptides less than 3 kDa. These peptides demonstrated cytotoxicity against HCT-116 cancer cells and inhibited cancer cell growth *in vitro* (Yaghoubzadeh et al., 2020). In another study, oyster peptides obtained by combined enzymatic hydrolysis of trypsin and alkaline protease exhibited inhibitory effect on B16 cell growth, where the peptide ILDSAPR inhibited B16 cell proliferation and promoted apoptosis by regulating the expression of B16 cell metabolism (Han et al., 2023). It was reported that the trypsin hydrolyzed fraction of MW $<$ 1 kDa, produced from the spinal cord of hybrid sturgeon (*Acipenseridae*), showed 34.84 $\pm$ 2.86% antiproliferative activity against HeLa cells at a concentration of 200 μg/mL. Additionally, this peptides fraction displayed a proliferative activity of 72.70 $\pm$ 2.46% on L929 cells, indicating no significant cytotoxicity (Han et al., 2022).

Thunnas albacares, also called tuna, is a highly nutritious marine fish species. However, the tuna fish trade industry generates nearly half of the total biomass in underutilized fish by-products (Martínez-Alvarez et al., 2015; Suo et al., 2022). Moreover, fish trade processing scraps (trimmings such as head, skin meat, viscera, *etc*.) are also abundant in high protein, polyunsaturated fatty acids, and other beneficial active substances that hold great potential for development and utilization (Idowu and Benjakul, 2019; Phadke et al., 2021). According to literature reports, the >2.5 kDa ultrafiltrated peptides fraction from tuna cooking solution was found to induce S-phase cell cycle arrest and apoptosis of MCF-7 cells by activating Caspase-related protein family (Hung et al., 2014). The purified polypeptide component from the enzymic hydrolysate of tuna dark muscle by-product showed an inhibitory effect on the proliferation of MCF-7 cells (Hsu et al., 2011). The characteristic sequences LPHVLTPEAGAT and PTAEGGVYMVT exhibited dose-dependent inhibition of MCF-7 cells with IC_{50} values of 8.1 and 8.8 μM, respectively. However, no conclusion has been drawn regarding whether amino acids contribute primarily to the antiproliferative activity of FPHs (Halim et al., 2016). And further research is warranted on the synergistic effect and the anti-tumor mechanism of tuna peptides in combination with chemotherapy drugs.

Currently, completely experimental methods for screening and identifying BP are time-consuming and resource-intensive tasks (Shoombuatong et al., 2018). However, the use of machine learning methods that employ bioinformatics techniques to analyze existing peptide databases for functional prediction of newly generated peptide sequences and analysis of protein structure and functional relationships can effectively improve the efficiency of mining novel BP (Peredo-Lovillo et al., 2022; G. Wang et al., 2022). Various computational methods have been developed for peptide activity prediction, utilizing a wide range of machine learning methods and peptide features, such as Ensemble-AMPPred (Lertampaiporn et al., 2021), ACPred (Schaduangrat et al., 2019), FIRM-AVP (Chowdhury et al., 2020), AntiFP (Agrawal et al., 2018), AIPred (Manavalan et al., 2018), dPABB (Sharma et al., 2016). The main modeling methods currently used for data classification include support vector machines, fuzzy K-nearest neighbors, discriminant analysis, generalized neural networks, probabilistic neural networks, homologous ensembles, random forests, and tree models (Lertampaiporn et al., 2021; Schaduangrat et al., 2019). Recently, a novel machine learning approach called CSM-PEPTIDES was propased, which explores the physicochemical properties, secondary structure of peptide sequences, and disordered regions to rapidly identify and predict eight different active peptides (Rodrigues et al., 2022). This method has been shown to outperform existing methods in active peptide exploration.

In this study, Tuna trimmings (*Thunnas albacares*) protein hydrolysate (TPA) was produced from tuna trimmings. The synergistic effect of varying doses of TPA in combination with 5-FU was evaluated, along with its potential for immune regulation and alleviation of intestinal mucosal injury in S180 tumor-bearing mouse models. Additionally, the amino acid composition and relative molecular weight distribution of TPA were analyzed, and the peptide sequence of TPA was identified. Database predictions were made regarding the anti-tumor and anti-inflammatory potential of TPA. These findings will provide important theoretical support for TPA as a valuable adjuvant therapy and nutritional ingredient in the chemotherapy of tumor patients' dietary needs.

2. Materials and methods

2.1. Materials

Tuna trimmings was obtained from Guangdong Xingyi Marine Bioengineering Co., Ltd. (Guangdong, China). Alcalase (400,000 U/g) was purchased from Pangbo Enzyme Co., Ltd. (Guangxi, China). Fluorouracil injection was obtained from Shanghai Xudong Haipu Pharmaceutical Co., Ltd (Production batch number: FA180121, Shanghai, China). Fetal bovine serum (FBS) was obtained from the Ritter Biotechnology Co., Ltd (Production batch number: S8056-01, Guangzhou, China); Trypan Blue was obtained from the Beijing Solaibao Technology Co. Ltd (Beijing, China); Dulbecco's modified Eagle's medium (DMEM) was obtained from Invitrogen Gibco (USA); Total Protein test Kit (biuret method), Albumin test kit (bromocresol green colorimetric method), Prealbumin test kit, Transferrin test kit, Immunoglobulin M test kit, Immunoglobulin G test kit, Immunoglobulin A test kit, Complement C3 test Kit and Complement C4 test Kit were all adopted immune turbidity method (Biosino Bio-Technology and Science Inc, Beijing). All other chemical reagents used were of analytical grade.

2.2. Preparation of TPA

The TPA was prepared according to the method of the previous study with slight modification (Cai et al., 2022). Tuna trimmings was blended with 3 vol of distilled water (w/v, g/mL) and stirred with a homogenizer to the minced homogenate without obvious particles. The homogenate solution was preheated to 50 °C in a 100 rpm thermostatic oscillator and adjusted to pH 8.0 with 1 M NaOH. Then the solution was hydrolyzed at 50 °C for 4 h with ratio of alcalase enzyme to substrate of 3000 u/g followed by enzyme-inactivation in boiling water bath for 10 min. After cooling, the enzymolysis solution was centrifuged at 8000 rpm (4 °C, 30 min). The supernatant was extracted and filtered with a 0.2 μm filter membrane, and the filtrate was lyophilized to obtain TPA.

2.3. In vivo experiment

2.3.1. Animals and experiments

Male BALB/c mice (25 $\pm$ 1 g) were obtained from the Laboratory Animal Medical Center of Sun Yat-Sen University (Certificate number: SCXK-2016-0029, Guangzhou, China), and were housed in standardized laboratory conditions of temperature (23 $\pm$ 1 °C), relative humidity (50 $\pm$ 5%) and an alternating 12 h light/dark cycle. All animal procedures were reviewed and approved by the Animal Ethics Committee of Sun Yat-sen University (Animal Ethics Approval Program Number: SYXK-2014-0020, Guangzhou, China)

Mouse sarcoma S180 cells were obtained from the Cell Bank of the Experimental Animal Center of Sun Yat-Sen University (Guangzhou, China). Referring to the modeling method of S180-bearing mice (Cai et al., 2021), S180 cells were adjusted to a cell concentration of 2.6 $\times$ 10^7 cells/ml of S180 single-cell suspension for subcutaneous injection, and 0.2 ml per cell was inoculated under the axilla of experimental mice. After 3 days, a cuticular layer tumor (about 2 mm $\times$ 2 mm) was visible in the groin of the mice, indicating that the model was successfully constructed. Mice

were randomly divided into 6 groups (n = 10), which were blank group, model group, 5-FU group (30 mg/kg, ip), L-TPA (200 mg/kg, ig) + 5-FU (30 mg/kg, ip) group, M-TPA (400 mg/kg, ig) + 5-FU (30 mg/kg, ip) group, and H-TPA (800 mg/kg, ig) + 5-FU (30 mg/kg, ip) group. The normal group and the model group were given normal saline daily (2 g/kg, ig), the 5-FU group was injected intraperitoneally (30 mg/kg, ip, once every two days), the combined group was given TPA (200 mg/kg, 400 mg/kg, 800 mg/kg, ig, once a day), and 5-FU (30 mg/kg, ip, once every two days) was injected intraperitoneally for 15 days.

2.3.2. Tumor suppression rate and serum biochemical analysis

The body weight of mice was recorded every 7 days during continuous dosing. At the same time, tumor size was calculated every 3 days using vernier calipers, including the length, width and height. The tumor volume (mm^3) was defined as length (mm) × width (mm) × height (mm)/2. After 24 h of dosing at the end of the experiment, blood was collected from the orbital vein, mice were sacrificed by necking, the tumor mass was stripped and the tumor suppression rate was calculated. Tumor suppression rate (%) = (1-tumor weight of the sample group/tumor weight of the model group) × 100% (Cai et al., 2021).

Mouse orbital blood collection 0.3 ml, using a hemocytometer to determine the blood routine of mice, including red blood cell count (RBC), white blood cell count (WBC), hematocrit (HCT), hemoglobin (HGB), total platelets (PLT), lymphocytes (LYM), monocytes (MONO), neutrophils (NEU), eosinophils (EOS), basophils (BASO). Serum was collected by centrifugation of the blood at 3000 rpm for 20 min. The serum concentrations of total protein (TP), immune globulin A, M, and G (IgA, IgM, and IgG), complement C3, complement C4, albumin (ALB), transferrin (TRF), prealbumin (PAB) were detected in serum according to the operation steps of each kit.

2.3.3. Histopathological examination

The small intestinal tissue was intercepted 2 cm, fixed by neutral formaldehyde, and paraffin-embedded, and after routine dehydration, hematoxylin-eosin (HE) staining was performed, and then the histological morphology of each layer of the mouse mucosa was observed by CX31 optical microscope (OLYMPUS, Japan). To quantitatively assess intestinal tissue, the average height of small intestinal villi, mean villi area, mean mucosal thickness, and crypt depth were measured using the Taimeng BI2000 image processing system (Chengdu Technology Market Co., Ltd., China).

2.4. Amino acid composition analysis of TPA

Acid hydrolysis: The TPA was accurately weighed into the hydrolysis tube, 6 M HCl was added, the tube was sealed, hydrolyzed at 110 °C for 22 h, cooled, constant volume, filtered, evaporated to remove excess hydrochloric acid, dissolved in 0.2 M sodium citrate buffer (pH 2.2), and analyzed by the amino acid analyzer (P.-Y. Wang et al., 2022). The analytical conditions were as follows: a 3 μM sulfonic acid cationic resin column of dimensions 4.6 × 60 mm was used, with column and reaction temperatures setting at 53 °C and 135 °C, respectively. The buffer solution and chromogenic agent solution were adjusted to flow at rates of 0.40 mL/min and 0.35 mL/min, respectively, and a 20 μL injection volume was used. The detection wavelengths were 570 nm for 32 min and 440 nm for 10 min.

The method for determination of tryptophan content was modified according to Çevikkalp et al. (2016). The TPA was accurately weighed into the hydrolysis tube, and 1.5 mL of 4 mol/L LiOH alkali hydrolytic agent was added, connected with the piston to evacuate the vacuum for about 10–15 min, sealed immediately, and hydrolyzed at 110 °C for 22 h. After the hydrolysis tube was cooled, the tube opening was cut, and the hydrolysis was transferred to a 50 mL volumetric flask with 0.2 M sodium citrate buffer (pH 2.2). Then 6 M HCl was added to neutralize it, and the volume was fixed with 0.2 M sodium citrate buffer (pH 2.2). The supernatant was filtered by a 0.45 μm filter membrane and analyzed by Agilent 1260 HPLC system (Agilent Technologies Hewlett-Packard-Strasse 8 76337 Waldbronn, Germany). The column was MN-C18, the mobile phase was 0.0085 M sodium acetate buffer and methanol (95:5), the flow rate was 1.0 ml/min, the wavelength was 280 nm, and the injection volume was: 20 μl.

2.5. Relative molecular weight distribution analysis of TPA

The experimental method is based on Wan et al. (2020). The concentration of the sample solution was 20 mg/mL. The molecular weight distribution of TPA was determined by Gel Permeation Chromatography (GPC) methods in Agilent 1260 HPLC system with the following conditions: TSKgel G2000SWXL column (300 mm × 7.8 mm, Tosoh Corporation, Japan); Mobile phase: 0.1% TFA-acetonitrile: 0.1% TFA-water = 20:80 (v/v), monitoring wavelength 220 nm, flow rate 0.5 mL/min, column temperature 35 °C, injection volume 5 μL. Cytochrome C (M:12355), aprotinin (M:6511), bacitracin (M:1422), L-oxidized glutathione (M:612.63) and phenylalanine (M:165.2) were used as relative molecular mass standards. The standard curve of log of molecular weight (logMw) and elution time (t) of the standard was $\log Mw = -0.0144t2+0.2552t+3.1123$ ($R^2 = 0.9991$).

2.6. Identification of amino acid sequences by LC-ESI-Q-TOF-MS/MS

Tuna hydrolysate peptide sequences were identified by LC-ESI-Q-TOF-MS/MS analysis on an HPLC system combined with a Bruker maXis Q-TOF Premier mass spectrometer (Bruker, Daltonik, GmbH, Bremen Germany) equipped with an electrospray ion source (ESI). The 20 μL sample was passed with a 0.22 μm membrane before being detected by the YMC-Pack ODS-AQ (250 × 4.6 mm, 5 μm) LC column. The elution condition for LC: eluent A consisted of 0.1% formic acid in deionized water, eluent B consisted of 0.1% formic acid in acetonitrile, the flow rate is set to 1 mL/min, and the detection wavelength is 220 nm. The elution procedure is as follows: 0–10 min, 8% B; 10–45 min, 30% B; 45–50 min, 90% B; 50–55 min, 8% B. The ESI system operates in positive mode and performs data acquisition by DIA with a capillary voltage of 3.8 kV and a scan range of 200–3000 m/z. All data acquisition and analysis were performed using PEAKS Studio 6.0 software (Bioinformatics Solutions Inc., Waterloo, Canada).

2.7. Database prediction of potential bioactivities

The physicochemical properties of the active peptides were then evaluated using ToxinPred (https://webs.iiitd.edu.in/raghava/toxinpred/index.html, Accessed, 2023/3/27) to analyze toxicity hydrophobicity, net charge, and PI isoelectric point.

Bioactivity prediction of peptide sequences assessed using CSM-Peptides (https://biosig.lab.uq.edu.au/csm_peptides, Accessed, 2023/2/7), using a score with the default cut-off value > 0.5 as the final prediction label and defined as a positive number.

2.8. Statistical analysis

All data were expressed as mean ± standard deviation (SD) and analyzed using SPSS 24.0 software (IBM Inc., New York, USA) by one-way analysis of variance (ANOVA) using Bonferroni's multi-range test. The results in $p < 0.05$ were considered statistically significant.

3. Results

3.1. Effects of TPA combined with 5-FU on body weight and tumors of tumor-bearing mice

The experimental results are shown in Table 1. Compared with 5-FU alone, the final body mass of mice in medium and high doses of TPA+5-FU groups increased ($p < 0.05$), indicating that medium and high dose

Table 1
Effects of different treatments on body weight, weight gain rate, tumor weight, and tumor inhibition rate of mice (mean ± SD, n = 10).

Constituencies	Administered dose(mg/kg)	Primary weight(g)	Final weight(g)	Weight gain rate(%)	Tumor weight(g)	Tumor suppression rate(%)
Normal	–	25.99 ± 1.23	29.11 ± 1.50	12.00	–	–
Model	–	24.27 ± 1.76	28.72 ± 2.51	18.34	1.57 ± 0.30	–
5-FU	30	24.14 ± 0.82	25.15 ± 1.41***	4.18	1.09 ± 0.16***	30.57
L-TPA+5-FU	200	24.25 ± 1.14	25.80 ± 1.36**	6.39	1.00 ± 0.32***	36.31
M-TPA+5-FU	400	25.18 ± 1.50	26.73 ± 1.56*#	6.16	0.92 ± 0.17***#	41.40
H-TPA+5-FU	800	24.56 ± 1.39	27.16 ± 1.92#	10.59	0.92 ± 0.36***	41.40

Note: *$p < 0.05$, **$p < 0.01$ and ***$p < 0.001$ compared with model group; #$p < 0.05$ compared with 5-FU group.

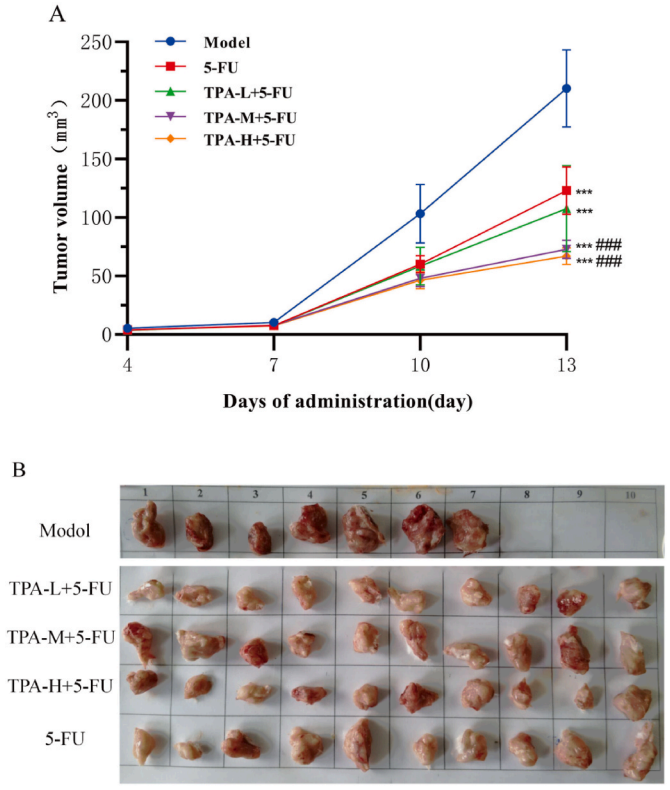

Fig. 1. Effects of different treatments on tumor growth of S180 tumor-bearing mice. (A). Change of tumor volume (mean ± SD, n = 10, ***$p < 0.001$ compared with model group; ###$p < 0.001$ compared with 5-FU group.) (B). Anatomical map of the tumor.

TPA may alleviate the consumption effect of the tumor on the body. Compared with the model group, 5-FU alone and TPA+5-FU treatment could significantly inhibit tumor growth, showing significant statistical significance ($p < 0.001$). Furthermore, the tumor weight in the medium-dose TPA+5-FU group was significantly lower than that in the 5-FU group ($p < 0.05$). The inhibitory rates for the TPA+5-FU groups at low, medium and high doses were 36%, 41% and 41% respectively, all of which were higher than that of the 5-FU group (31%).

Fig. 1A and B indicate that both 5-FU and TPA+5-FU effectively suppress tumor growth in mice. On day 13, the medium and high doses of TPA+5-FU administration demonstrated a significant reduction in tumor volume compared to the model group and 5-FU group ($p < 0.001$, $p < 0.001$), which shows a synergistic inhibitory effect on tumor growth.

3.2. Protective effect of TPA on intestinal mucosa

As shown in Fig. 2A, small intestinal mucosa in the 5-FU group shows microscopic signs of atrophic degeneration and necrotic detachment, leading to a significant expansion of the glandular lumen. The venous plexus is significantly congested and dilated with visible hemorrhage, accompanied by increased inflammatory cell infiltration. Indicators such as the height of villi, the number of crypt foci, the thickness of the mucous membrane and the area of the villi are significantly reduced. Meanwhile, as shown in Fig. 2B–E, the small intestinal villi height, villi surface area, and mucosal layer width of mice in the 5-FU group were significantly reduced compared to the model group ($p < 0.001$).

The combination of TPA and 5-FU resulted in normal histomorphology changes in the small intestine and substantially reduced the intestinal mucosal injury induced by 5-FU. Referencing Fig. 2B through 2E, in all observed indices pertaining to the histopathology of the small intestine, the low, medium, and high dose TPA+5-FU groups exhibited significant increases in comparison to the 5-FU group ($p < 0.05$). Furthermore, the villi area significantly increased in the low and high dose groups, while the villi height, crypt depth, and mucosal thickness significantly increased in the medium and high dose TPA+5-FU groups with statistical significance ($p < 0.001$). As such, these findings commend the combination of TPA with 5-FU may alleviate 5-FU induced intestinal mucosal injury.

3.3. Effect of TPA on peripheral blood routine in tumor-bearing mice

As shown in Table 2, the whole blood of the mice undergoes significant changes after the tumor cells transplant. Compared with the normal group, WBC, NEU and MONO in the model group were increased ($p < 0.001$), and LYM was decreased ($p < 0.001$) and EOS was decreased ($p < 0.01$), indicating that the tumor caused the body to produce an inflammatory response and caused a decrease in the body's immune function. In addition, RBC, HGB and HCT were decreased and had a significant effect ($p < 0.001$) and PLT was significantly increased ($p < 0.001$) suggesting that tumorigenesis causes anemia in mice.

Compared with the model group, WBC was remarkedly lower in the treatment with 5-FU alone ($p < 0.001$), and there was no differential change in other indexes ($p > 0.05$), but under combined treatment, WBC was significantly lower in S180 tumor-bearing mice in the low, medium and high dose TPA+5-FU groups ($p < 0.001$). LYM was increased in the low and medium dose groups ($p < 0.001$), and NEU was decreased ($p < 0.001$), MONO was decreased in both medium and high dose groups ($p < 0.05$), suggesting that TPA combined with 5-FU dosing could alleviate the occurrence of inflammatory response and improve immune depression in mice. However, RBC was reduced ($p < 0.05$) and HCT was reduced ($p < 0.01$) in the low and medium dose groups compared to the model group, while HGB was reduced ($p < 0.05$) in the low dose, and HCT was reduced ($p < 0.05$) in the low dose group compared to the 5-FU group, and PLT was increased ($p < 0.05$) in the low versus high dose groups. It is suggested that the combination of TPA and 5-FU has a weak effect on the improvement of tumor-induced anemia *in vivo*.

3.4. Effect of TPA on serum biochemical indexes of tumor-bearing mice

As shown in Table 3, the results indicated that the 5-FU group interfered with the normal nutrient metabolism and immune function of the organism, resulting in a significant decrease in ALB and C4 levels ($p < 0.01$).

In the low, medium, and high dose TPA+5-FU groups, the TP had a significant increase compared to the model group ($p < 0.01$, $p < 0.01$, p

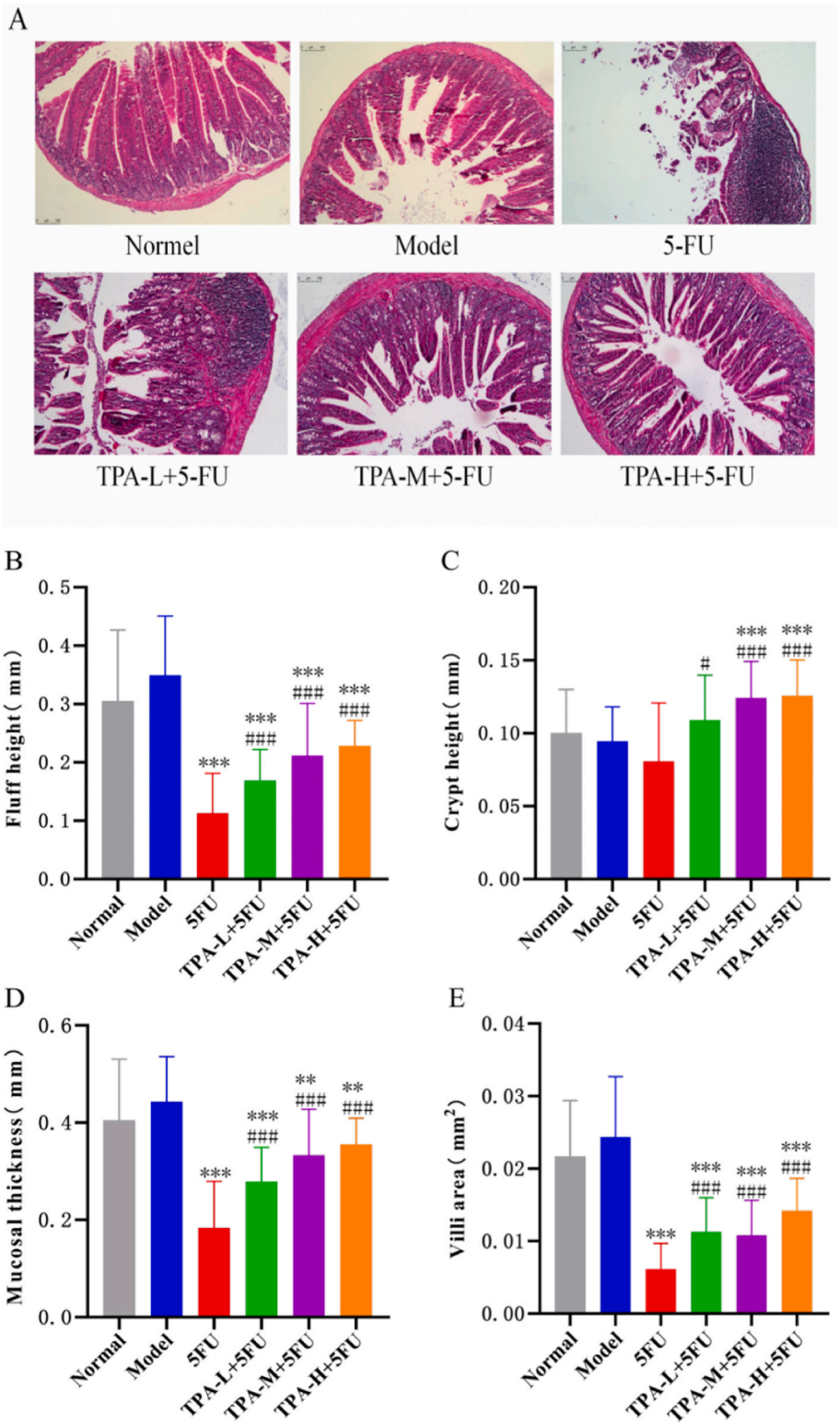

Fig. 2. Protective effect of TPA combined with 5-FU on intestinal mucosa injury. Histopathological staining of the small intestine (magnification 10×) (A); Histomorphological analyses of the Villus height(B), Crypt depth(C), mucosa thickness(D), and Villus surface area(E). $^{**}p < 0.01$ and $^{***}p < 0.001$ compared with model group; $\#p < 0.05$ and $\#\#\#p < 0.001$ compared with 5-FU group.

Table 2
Effects of different treatments on blood routine exam of mice(mean ± SD, n = 10).

Group	Normal	Model	5-FU	TPA-L+5-FU	TPA-M+5-FU	TPA-H+5-FU
WBC(× 10^9/L)	6.61 ± 2.58***	13.22 ± 3.23	4.71 ± 0.99***	4.77 ± 0.60***	5.31 ± 0.93***	5.16 ± 0.96***
LYM(%)	80.29 ± 4.17***	54.82 ± 6.35	62.65 ± 11.25	72.45 ± 11.29***	69.70 ± 7.27***	62.94 ± 7.26*
NEU(%)	17.47 ± 4.08***	39.43 ± 6.90	32.14 ± 9.61	23.15 ± 9.66***	26.03 ± 7.31***	32.74 ± 6.33*
MONO(%)	0.87 ± 0.43***	4.98 ± 1.57	4.22 ± 2.22	3.66 ± 2.01	3.40 ± 1.11*	3.34 ± 1.63*
EOS(%)	1.34 ± 0.45**	0.74 ± 0.19	0.99 ± 0.51	0.72 ± 0.52	0.87 ± 0.37	0.96 ± 0.50
BASO(%)	0.030 ± 0.067	0.030 ± 0.048	0.000 ± 0.000	0.020 ± 0.063	0.000 ± 0.000###	0.020 ± 0.042
RBC(× 10^{12}/L)	10.34 ± 0.46***	9.03 ± 0.37	8.82 ± 0.44	8.71 ± 0.36*	8.60 ± 0.35*	8.60 ± 0.34
HGB(g/L)	158.9 ± 6.7***	136.2 ± 6.2	134.7 ± 5.6	130.1 ± 4.7*	131.0 ± 5.1	133.8 ± 5.1
HCT(%)	44.9 ± 1.68***	39.1 ± 1.27	38.5 ± 1.60	37.1 ± 1.15**#	37.2 ± 1.18**	38.2 ± 1.28
PLT(× 10^9/L)	1312.3 ± 149.9***	1740.9 ± 169.8	1601.5 ± 196.8	1767.0 ± 116.1#	1657.0 ± 162.9	1783.9 ± 146.7#

Note: *$p < 0.05$, **$p < 0.01$ and ***$p < 0.001$ compared with model group; #$p < 0.05$ and ###$p < 0.001$ compared with 5-FU group.

Table 3
Effects of different treatments on serum biochemical indicators of mice(mean ± SD, n = 10).

Group	Normal	Model	5-FU	TPA-L+5-FU	TPA-M+5-FU	TPA-H+5-FU
TP(g/L)	73.83 ± 7.65***	57.35 ± 7.11	54.72 ± 6.55	67.97 ± 6.25**###	68.10 ± 7.04**###	65.28 ± 6.97*##
ALB(g/L)	48.41 ± 4.62***	36.15 ± 5.41	29.90 ± 3.23**	38.27 ± 5.26###	39.10 ± 4.81###	41.28 ± 5.64###
C3(g/L)	2.555 ± 0.611***	3.785 ± 0.408	3.092 ± 1.124	3.635 ± 0.921	3.883 ± 0.776	3.761 ± 0.826
C4(g/L)	0.376 ± 0.072***	0.528 ± 0.064	0.403 ± 0.079**	0.446 ± 0.085*	0.424 ± 0.075**	0.452 ± 0.061*
IgA(g/L)	0.371 ± 0.125***	0.133 ± 0.031	0.121 ± 0.031	0.129 ± 0.044	0.143 ± 0.031	0.141 ± 0.030
IgG(g/L)	13.54 ± 1.98**	10.57 ± 2.06	10.12 ± 0.98	10.64 ± 1.58	10.75 ± 1.31	10.60 ± 1.80
IgM(g/L)	1.715 ± 0.327***	1.081 ± 0.194	0.992 ± 0.152	1.026 ± 0.177	1.139 ± 0.233	1.398 ± 0.344*##
PAB(mg/L)	3.74 ± 0.70**	2.71 ± 0.53	2.45 ± 0.46	2.94 ± 0.58	2.91 ± 0.59	3.06 ± 0.55#
TRF(g/L)	10.31 ± 1.54**	8.52 ± 1.08	8.64 ± 1.21	9.23 ± 1.12	9.25 ± 1.35	9.58 ± 1.53

Note: *$p < 0.05$, **$p < 0.01$ and ***$p < 0.001$ compared with model group; #$p < 0.05$, ##$p < 0.01$ and ###$p < 0.001$ compared with 5-FU group.

< 0.05). There was also noteworthy increase compared with the 5-FU group ($p < 0.001$, $p < 0.001$, $p < 0.01$), and the ALB was significantly increased by TPA ($p < 0.001$), indicating that the combination of TPA and 5-FU could improve the energy expenditure of the body, which was better than the effect of 5-FU alone. Besides, IgM levels in the high dose TPA+5-FU group were increased compared with the model group and the 5-FU group ($p < 0.05$, $p < 0.01$). In addition, the PAB was increased compared with 5-FU during the same period, with significant differences between them ($p < 0.05$). The above results support that TPA has a moderating effect on the serum antibody levels in tumor-bearing mice and can alleviate the interference of 5-FU with the normal nutrient metabolism and immune function of the organism.

3.5. Amino-acid composition and peptides profile analysis of TPA

Table 4 provides insight into the amino acid composition and content of TPA. TPA consists of 66.30 g/100 g amino acids, whereby essential amino acids amount to 30.36 g/100 g. Among the 17 distinct amino acids, glutamic acid is present with the highest concentration (10.06 g/100 g), followed by aspartic acid (6.78 g/100 g) (supplementary data Figs. S1–S7 and Table S1-S6).

Table 4
Amino acid composition of TPA.

Amino acid species	Amino acid content(g/100 g)	Amino acid species	Amino acid content(g/100 g)
Asp	6.78	Leu*	4.87
Thr*	3.21	Tyr	2.12
Ser	2.73	Phe*	2.46
Glu	10.06	Lys*	6.00
Pro	2.30	His*	5.37
Gly	3.48	Arg	3.61
Ala	4.39	Trp*	0.78
Val*	3.46	Total amino acid (TAA)	66.30
Met*	1.96	Essential amino acid content (EAA)	30.36
Ile*	2.73	EAA/TAA (%)	45.80

Note: * is an essential amino acid.

Table 5
Percentage of peak area of different molecular weight ranges in TPA (%).

Range of molecular weight (kDa)	Peak area	Percentage of integrated peak area (%)
>1 kDa	8635.1	11.46
1–0.25 kDa	48625.5	64.54
<0.25 kDa	18084.2	24.00

Tuna trimmings is rich in protein that can be prepared into small-molecular peptides and oligopeptides by enzymatic hydrolysis. As shown in Table 5, the molecular weight distribution of TPA peptides in the range 0.25–1 kDa was account for 64.54%. These results indicated that the tuna trimmings treated with alcalase was mainly composed of small-molecule peptides or oligopeptides (supplementary data Fig. S8-S9).

3.6. Identification of peptides in TPA

The peptide sequences of TPA were identified by HPLC-ESI-Q-TOF-MS/MS. As shown in Table 6, the 109 peptide sequences with 7–21 amino acids per peptide and molecular weights in the range of 648–2096 Da were identified according to the −10lgP value ≥ 15 (supplementary data Figs. S10–S119 and Table S7).

3.7. The anticancer and anti-inflammatory potentiality prediction

The total of 109 peptide sequences were predicted in the CSM-PEPTIDES database. The results showed that 68 peptides were described to possess anti-cancer activity with scores between 0.50 and 0.78. And 77 peptides were described to have anti-inflammatory activity with prediction scores between 0.50 and 0.90 (supplementary data Table. S8). The CSM-PEPTIDES database predicted anti-inflammatory peptides with scores >0.8 and anti-cancer peptides with scores >0.7 was shown in Table 6.

Table 6
Sequence information of anti-inflammatory peptides with predicted scores >0.8 and anti-cancer peptides with scores >0.7

Number	Peptide sequence	Mol wt	Anti-Inflammatory[a]	Toxicity[b]	Hydrophobicity[b]	Charge[b]	pI[b]
26	***GMDVINM***	***779.04***	***0.98***	***Non-Toxin***	***0.08***	***−1.00***	***3.80***
101	NNNHLDDI	954.08	0.98	Non-Toxin	−0.31	−1.50	4.20
36	SHPDLNVV	880.08	*0.94*	Non-Toxin	−0.06	−0.50	5.09
44	QPMEYACYPQ	1229.52	0.93	Non-Toxin	−0.15	−1.00	4.00
88	VPIPVPLPM	962.39	0.93	Non-Toxin	0.26	0.00	5.88
98	GIPLIKAD	826.12	0.90	Non-Toxin	0.06	0.00	6.19
43	SFVAGEAY	843.00	0.87	Non-Toxin	0.12	−1.00	4.00
109	ALPEMLPY	933.24	0.87	Non-Toxin	0.10	−1.00	4.00
17	***VMAPGAGVY***	***864.15***	***0.86***	***Non-Toxin***	***0.23***	***0.00***	***5.88***
86	WITYGPV	764.93	0.84	Non-Toxin	0.04	−1.00	3.80
41	AINDPFIDL	1017.27	0.83	Non-Toxin	0.08	−2.00	3.57
57	IVPIVEPE	895.18	0.83	Non-Toxin	0.14	−2.00	3.80
58	LVPIVEPE	895.18	0.83	Non-Toxin	0.12	−2.00	3.80
67	FMAYYPIE	1033.31	0.82	Non-Toxin	0.15	−1.00	4.00
91	MGDVLASC	795.04	0.82	Non-Toxin	0.10	−1.00	3.80
95	WEPPIID	869.08	0.82	Non-Toxin	0.05	−2.00	3.67
64	DTGIQASHPDLNVVGGASF	1885.30	0.81	Non-Toxin	0.00	−1.50	4.20
28	AQTVPYGIPLIK	874.02	*0.80*	Non-Toxin	−0.11	−2.00	3.57
Number	**Peptide sequence**	**Mol wt**	**Anti-Cancer[a]**	**Toxicity[b]**	**Hydrophobicity[b]**	**Charge[b]**	**pI[b]**
90	VLDTGIQA	816.04	0.78	Non-Toxin	0.08	−1.00	3.80
8	EVMAPGAGVY	993.28	*0.75*	Non-Toxin	0.15	−1.00	4.00
62	KYDSVIAV	894.14	0.74	Non-Toxin	0.00	0.00	6.18
26	***GMDVINM***	***779.04***	***0.73***	***Non-Toxin***	***0.08***	***−1.00***	***3.80***
108	EKAASFDIP	977.19	0.73	Non-Toxin	−0.10	−1.00	4.38
17	***VMAPGAGVY***	***864.15***	***0.72***	***Non-Toxin***	***0.23***	***0.00***	***5.88***
45	KYDSVIAVG	951.21	0.70	Non-Toxin	0.02	0.00	6.18
74	KYDSVIAVGA	1022.30	0.70	Non-Toxin	0.04	0.00	6.18

Note: a: according to "CSM-PEPTIDES"(https://biosig.lab.uq.edu.au/csm_peptides); b: according to "Toxinpred"(https://webs.iiitd.edu.in/raghava/toxinpred/index.html).

4. Discussion

After day 7, tumor cells rapidly proliferate, resulting in a larger tumor volume and an increased proportion of tumor mass in the model group of mice. This has a significant impact on body weight, mobility, and mental status. Although 5-FU is an analogue of uracil that can effectively interfere with the function of thymidylate synthase (TS) to inhibit tumor cell multiplication, its toxicity to normal tissues and the development of tumor resistance limits the success of cancer chemotherapy (Lee et al., 2014; Moutabian et al., 2022). Combining natural active ingredients with chemotherapeutic drugs can have multiple benefits, including synergistic anti-tumor effects that can inhibit tumor multidrug resistance, reduce the side effects of chemotherapeutic drugs, and regulate immune function. This approach may become a new strategy for clinical treatment of tumors (Li et al., 2022). In this experiment, the low, medium, and high dose TPA+5-FU combination groups (with tumor inhibition rates of 36%, 41%, and 41%, respectively) showed better results than the group treated with 5-FU alone (31%) in terms of inhibiting tumor cell growth. This indicates that there is a significant auxiliary effect in the treatment process of TPA combined with 5-FU chemotherapy.

During treatment with 5-FU chemotherapy, intestinal mucosal damage occurs which is characterized by an increase in crypt apoptosis and villi atrophy (Sougiannis et al., 2019; Liu et al., 2021). This leaves the mucosal tissue vulnerable to infection and ulceration (Taieb et al., 2014; Gelen et al., 2018). Furthermore, 5-FU treatment also leads to oxidative stress in the body, leading to a pro-inflammatory response that activates the production of nuclear factor NF-κB mediated pro-inflammatory cytokines, such as tumor necrosis factor (TNF), interleukin-6 (IL-6) and interleukin-1β (IL-1β) (Cinausero et al., 2017). Subsequently, this results in apoptosis, atrophy, ulceration, and inflammation in the gastrointestinal tract. In addition, a related study found that tuna bioactive peptide (TBP) significantly alleviated colitis symptoms (Xiang et al., 2021). The TBP improved body weight and disease activity index (DAI score), inhibited pro-inflammatory cytokine production, attenuated colonic tissue damage, restored disturbed intestinal flora, and increased short-chain fatty acid production. In the current trial, it was found that the combination of TPA and 5-FU dosing enhanced tumor suppression while limiting injury to the intestinal mucosal structures in S180 tumor-bearing mice when compared to using only 5-FU monotherapy. Moreover, the use of TPA led to the improvement of the intestinal mucosal structures and even tended to restore them to normal levels with increasing TPA content. Therefore, TPA qualifies as an adjuvant enteral nutrition agent that can improve immune depression and intestinal mucosal damage induced by 5-FU during chemotherapy while also regulating the nutritional level in post-operative chemotherapy patients.

The chemotherapy drug 5-FU is known to have direct or indirect effects on immune cell-mediated responses such as T cells, natural killer cells, and bone marrow-derived suppressor cells (Cinausero et al., 2017; Ghiringhelli and Apetoh., 2015). Its non-selective nature causes anti-tumor effects while affecting circulating myeloid cells, lymphocytes, and the immune response of the organism. Additionally, 5-FU can inhibit peripheral blood mononuclear cell activation and proliferation, leading to impaired immune function. It not only causes a decrease in the number of peripheral blood mononuclear cells, but also increasing the frequency of Treg cells to weaken T cell-mediated immunity against malignant tumors, thereby suppressing anti-tumor effector T cell function. (Tohyama et al., 2013). In an analysis evaluating enteral nutrition with concurrent radiation therapy (CCRT), researchers found that Enteral nutrition maintained albumin and total protein levels at the normal level. (Qiu et al., 2020). Peptide-based formulas are more easily digestible for patients with malabsorption or proven gastrointestinal intolerance to standard formulas since proteins are hydrolyzed into short peptides (Doley, 2022). Studies of enteral nutrition regarding immunomodulatory formulations have shown improvements in the prognostic treatment of trauma and surgical Intensive Care Unit patients, such as reduced infection rates, shorter length of stay, and shorter duration of mechanical ventilation, suggesting that some peptide-based enteral nutrition formulations are considered immune enhancing or immunomodulatory (McClave et al., 2016). In this study, the use of TPA combined with 5-FU significantly reduced leukocyte content in whole

blood while increasing secretion of lymphocytes and monocytes, suggesting that TPA can inhibit massive secretion of inflammatory cells caused by 5-FU treatment, enhancing immune function. Furthermore, in serum biochemical analysis for mice, TPA showed improvement in the total protein and albumin content of organisms, but a slight increase, not significant ($p > 0.05$), affecting secretion of C3, C4, IgA, and IgG, with only IgM being significant in the high-dose group ($p < 0.01$). This suggests that TPA may exhibit adjuvant antitumor effect by reducing protein depletion in the body and improving nutritional status.

Amino acids form the fundamental building blocks of protein composition and play a crucial role in the body's immune system by engaging in the body's inflammatory and immune responses. Among these, glutamate has been observed to provide energy to intestinal epithelial cells in mammals through mitochondrial oxidation (Li et al., 2016), promoting cell proliferation while reducing mucositis caused by 5-FU by inhibiting apoptosis and enhancing cell proliferation (Jonan et al., 2022). Aspartic acid can reduce intestinal damage and improve intestinal energy status (Pi et al., 2014). The experiment demonstrated that TPA contains a considerable amount of total amino acids (66.30 g/100 g), with glutamic acid present at high levels (10.06 g/100 g), and the peptides are primarily composed of small molecules and oligopeptides below 1 kDa, indicating superior absorption by the body. These findings suggest that the biological activity of TPA may be associated with its amino acid content and peptides composition.

The physicochemical characteristics of a peptide sequence, such as amino acid composition, hydrophobicity, secondary structure and net charge, may be linked to its antitumor activity (Chiangjong et al., 2020; Roudi et al., 2017). Hydrophobicity and secondary structure play essential roles in the anticancer properties of peptides. Significantly, peptides with higher hydrophobicity and α-helical structure exhibit an increased anticancer effect (Schaduangrat et al., 2019). Additionally, dimeric and tetrameric peptides possess enhanced cytotoxicity against cancer cells (Vargas Casanova et al., 2017), and peptide aggregation represents an intriguing approach to amphipathic membrane disruption (Nyström and Malmsten, 2018). The majority (55.96%) of peptide sequences in TPA display hydrophobicity, with glycine, lysine, and leucine residues serving as characteristic amino acids for functional assessment of anticancer peptides (Shoombuatong et al., 2018). Notably, most identified peptide sequences encompass these specific amino acids. CSM-PEPTIDES predicted the potential biological activity of TPA peptide sequences, identifying 68 out of 109 peptides as anti-tumor and 77 peptides as anti-inflammatory. These database predictions suggest that the antitumor and immunomodulatory effects of TPA in combination with 5-FU could relate to the peptide sequence composition in TPA.

5. Conclusion

In conclusion, the combination of TPA and 5-FU can enhance the suppression rate of tumors, mitigate the mucosal damage induced by 5-FU in the intestines, and maintain the normal morphology of the villi and crypt structures in the small intestinal mucosa. TPA can improve the nutritional and survival status of the body, as manifested by increased levels of serum total protein, albumin, and immunoglobulin, which reduces protein loss and energy consumption, thus boosting the overall health of the body. The peptide sequence composition of TPA may also contribute to its synergistic anti-tumor effects with 5-FU and immunomodulatory effects on the body. However, further research is required to screen active peptide sequences, and establish its mechanism of action to gain a better understanding of the effects of TPA on the intestines and the immune system in chemotherapy-induced damage.

CRediT authorship contribution statement

Xiangtan Zhao: Conceptualization, Investigation, Formal analysis, Methodology, Data curation, Writing – original draft. **Bingna Cai:** Methodology, Investigation, Validation. **Hua Chen:** Methodology, Investigation. **Peng Wan:** Resources, Validation, Investigation. **Deke Chen:** Resources, Investigation, Visualization. **Ziqing Ye:** Formal analysis, Software, Methodology. **Ailing Duan:** Investigation, Visualization. **Xin Chen:** Resources, Software. **Huili Sun:** Funding acquisition, Project administration, Supervision. **Jianyu Pan:** Writing – review & editing, Conceptualization, Funding acquisition, Project administration, Supervision.

Declaration of competing interest

The authors declare that they have no known competing financial interests or personal relationships that could have appeared to influence the work reported in this paper.

Data availability

The data that has been used is confidential.

Acknowledgments

The authors are indebted to Dr. Shikun Dai, engineer Yun Zhang and Aijun Sun (the Equipment Public Service Center, SCSIO, CAS) for their assistance with the high-speed refrigerated centrifuge and mass spectrometric analysis. This research was supported by the Key-Area Research and Development Program of Guangdong Province (No. 2020B1111030004), the Marine Economic Development Project (No. GDNRC[2022]36, GDNRC [2023]38), the Institution of South China Sea Ecology and Environmental Engineering, Chinese Academy of Sciences (No. ISEE2021PY05), the Key Research and Development Program of Hainan Province (No. ZDYF2021SHFZ109), the National Natural Science Foundation of Guangdong (No. 2022A1515010767) and the Department of Education of Guangdong Province (2021KTSCX114).

Appendix A. Supplementary data

Supplementary data to this article can be found online at https://doi.org/10.1016/j.crfs.2023.100547.

References

Agrawal, P., Bhalla, S., Chaudhary, K., Kumar, R., Sharma, M., Raghava, G.P., 2018. In silico approach for prediction of antifungal peptides. Front. Microbiol. 9, 323. https://doi.org/10.3389/fmicb.2018.00323.

Cai, B., Pan, J., Chen, H., Chen, X., Ye, Z., Yuan, H., Sun, H., Wan, P., 2021. Oyster polysaccharides ameliorate intestinal mucositis and improve metabolism in 5-fluorouracil-treated s180 tumour-bearing mice. Carbohydrate Polym. 256, 117545 https://doi.org/10.1016/j.carbpol.2020.117545.

Cai, B., Wan, P., Chen, H., Huang, J., Ye, Z., Chen, D., Pan, J., 2022. Purification and identification of novel myeloperoxidase inhibitory antioxidant peptides from tuna (*Thunnas albacares*) protein hydrolysates. Molecules 27 (9), 2681. https://doi.org/10.3390/molecules27092681.

Çevikkalp, S.A., Löker, G.B., Yaman, M., Amoutzopoulos, B., 2016. A simplified hplc method for determination of tryptophan in some cereals and legumes. Food Chem. 193, 26–29. https://doi.org/10.1016/j.foodchem.2015.02.108.

Chakniramol, S., Wierschem, A., Cho, M.-G., Bashir, K.M.I., 2022. Physiological and clinical aspects of bioactive peptides from marine animals. Antioxidants 11 (5), 1021. https://doi.org/10.3390/antiox11051021.

Chakrabarti, S., Jahandideh, F., Wu, J., 2014. Food-derived bioactive peptides on inflammation and oxidative stress. BioMed Res. Int. https://doi.org/10.1155/2014/608979, 2014.

Chiangjong, W., Chutipongtanate, S., Hongeng, S., 2020. Anticancer peptide: physicochemical property, functional aspect and trend in clinical application. Int. J. Oncol. 57 (3), 678–696. https://doi.org/10.1038/s41598-020-76161-8.

Chowdhury, A.S., Reehl, S.M., Kehn-Hall, K., Bishop, B., Webb-Robertson, B.-J.M., 2020. Better understanding and prediction of antiviral peptides through primary and secondary structure feature importance. Sci. Rep. 10 (1), 19260 https://doi.org/10.1038/s41598-020-76161-8.

Cinausero, M., Aprile, G., Ermacora, P., Basile, D., Vitale, M.G., Fanotto, V., Parisi, G., Calvetti, L., Sonis, S.T., 2017. New frontiers in the pathobiology and treatment of cancer regimen-related mucosal injury. Front. Pharmacol. 8, 354. https://doi.org/10.3389/fphar.2017.00354.

Cipolari, O.C., de Oliveira Neto, X.A., Conceição, K., 2020. Fish bioactive peptides: a systematic review focused on sting and skin. Aquaculture 515, 734598. https://doi.org/10.1016/j.aquaculture.2019.734598.

Daroit, D.J., Brandelli, A., 2021. In vivo bioactivities of food protein-derived peptides–a current review. Curr. Opin. Food Sci. 39, 120–129. https://doi.org/10.1016/j.cofs.2021.01.002.

Doley, J., 2022. Enteral nutrition overview. Nutrients 14 (11), 2180. https://doi.org/10.3390/nu14112180.

Gelen, V., Şengül, E., Yıldırım, S., Atila, G., 2018. The protective effects of naringin against 5-fluorouracil-induced hepatotoxicity and nephrotoxicity in rats. Iranian J. Basic Med. Sci. 21 (4), 404. https://doi.org/10.22038/ijbms.2018.27510.6714.

Ghiringhelli, F., Apetoh, L., 2015. Enhancing the anticancer effects of 5-fluorouracil: current challenges and future perspectives. Biomed. J. 38 (2) https://doi.org/10.4103/2319-4170.130923.

Halim, N., Yusof, H., Sarbon, N., 2016. Functional and bioactive properties of fish protein hydolysates and peptides: a comprehensive review. Trends Food Sci. Technol. 51, 24–33. https://doi.org/10.1016/j.tifs.2016.02.007.

Han, G., Wang, J., Li, Y., Chen, Z., Xu, X., Liu, T., Wang, Y., Bai, F., Liu, K., Zhao, Y., 2022. Novel peptide from the hydrolysate of hybrid sturgeon (acipenseridae) spinal cord: isolation, identification, and anti-proliferative effects in human cervix cancer cells. J. Agric. Food Chem. https://doi.org/10.1021/acs.jafc.2c07594.

Han, J., Geng, L., Lu, C., Zhou, J., Li, Y., Ming, T., Zhang, Z., Su, X., 2023. Analyzing the mechanism by which oyster peptides target il-2 in melanoma cell apoptosis based on rna-seq and m6a-seq. Food Funct. 14 (5), 2362–2373. https://doi.org/10.1039/d2fo03672j.

Houyvet, B., Bouchon-Navaro, Y., Bouchon, C., Goux, D., Bernay, B., Corre, E., Zatylny-Gaudin, C., 2018. Identification of a moronecidin-like antimicrobial peptide in the venomous fish pterois volitans: functional and structural study of pteroicidin-α. Fish Shellfish Immunol. 72, 318–324. https://doi.org/10.1016/j.fsi.2017.11.003.

Hsu, K.-C., Li-Chan, E.C., Jao, C.-L., 2011. Antiproliferative activity of peptides prepared from enzymatic hydrolysates of tuna dark muscle on human breast cancer cell line mcf-7. Food Chem. 126 (2), 617–622. https://doi.org/10.1016/j.foodchem.2010.11.066.

Hung, C.-C., Yang, Y.-H., Kuo, P.-F., Hsu, K.-C., 2014. Protein hydrolysates from tuna cooking juice inhibit cell growth and induce apoptosis of human breast cancer cell line mcf-7. J. Funct.Foods 11, 563–570. https://doi.org/10.1016/j.jff.2014.08.015.

Idowu, A.T., Benjakul, S., 2019. Bitterness of fish protein hydrolysate and its debittering prospects. J. Food Biochem. 43 (9), e12978 https://doi.org/10.1111/jfbc.12978.

Idowu, A.T., Benjakul, S., Sinthusamran, S., Pongsetkul, J., Sae-Leaw, T., Sookchoo, P., 2019. Whole wheat cracker fortified with biocalcium and protein hydrolysate powders from salmon frame: characteristics and nutritional value. Food Quality and Safety 3 (3), 191–199. https://doi.org/10.1093/fqsafe/fyz012.

Jonan, S., Hamouda, N., Fujiwara, A., Iwata, K., Fujita, T., Kato, S., Amagase, K., 2022. Alleviative effects of glutamate against chemotherapeutic agent-induced intestinal mucositis. J. Physiol. 73 (4) https://doi.org/10.1093/fqsafe/fyz012.

Kundam, D.N., Acham, I.O., Girgih, A.T., 2018. Bioactive compounds in fish and their health benefits. Asian Food Sci. J. 4 (4), 1–14. https://doi.org/10.9734/AFSJ/2018/41803.

Lee, C.S., Ryan, E.J., Doherty, G.A., 2014. Gastro-intestinal toxicity of chemotherapeutics in colorectal cancer: the role of inflammation. World J. Gastroenterol.: WJG 20 (14), 3751. https://doi.org/10.3748/2Fwjg.v20.i14.3751.

Lertampaiporn, S., Vorapreeda, T., Hongsthong, A., Thammarongtham, C., 2021. Ensemble-amppred: robust amp prediction and recognition using the ensemble learning method with a new hybrid feature for differentiating amps. Genes 12 (2), 137. https://doi.org/10.3390/genes12020137.

Li, B., Shao, H., Gao, L., Li, H., Sheng, H., Zhu, L., 2022. Nano-drug co-delivery system of natural active ingredients and chemotherapy drugs for cancer treatment: a review. Drug Deliv. 29 (1), 2130–2161. https://doi.org/10.1080/10717544.2022.2094498.

Li, X.-G., Sui, W.-G., Gao, C.-Q., Yan, H.-C., Yin, Y.-L., Li, H.-C., Wang, X.-Q., 2016. L-glutamate deficiency can trigger proliferation inhibition via down regulation of the mtor/s6k1 pathway in pig intestinal epithelial cells. J. Anim. Sci. 94 (4), 1541–1549. https://doi.org/10.2527/jas.2015-9432.

Liu, J.-H., Hsieh, C.-H., Liu, C.-Y., Chang, C.-W., Chen, Y.-J., Tsai, T.-H., 2021. Anti-inflammatory effects of radix aucklandiae herbal preparation ameliorate intestinal mucositis induced by 5-fluorouracil in mice. J. Ethnopharmacol. 271, 113912 https://doi.org/10.1016/j.jep.2021.113912.

Manavalan, B., Shin, T.H., Kim, M.O., Lee, G., 2018. Aippred: sequence-based prediction of anti-inflammatory peptides using random forest. Front. Pharmacol. 9, 276. https://doi.org/10.3389/fphar.2018.00276.

Martínez-Alvarez, O., Chamorro, S., Brenes, A., 2015. Protein hydrolysates from animal processing by-products as a source of bioactive molecules with interest in animal feeding: a review. Food Res. Int. 73, 204–212. https://doi.org/10.1016/j.foodres.2015.04.005.

McClave, S.A., Taylor, B.E., Martindale, R.G., Warren, M.M., Johnson, D.R., Braunschweig, C., McCarthy, M.S., Davanos, E., Rice, T.W., Cresci, G.A., 2016. Guidelines for the provision and assessment of nutrition support therapy in the adult critically ill patient: society of critical care medicine (sccm) and american society for parenteral and enteral nutrition (aspen). J. Parenteral Enteral Nutr. 40 (2), 159–211. https://doi.org/10.1177/0148607115621863.

Moutabian, H., Majdaeen, M., Ghahramani-Asl, R., Yadollahi, M., Gharepapagh, E., Ataei, G., Falahatpour, Z., Bagheri, H., Farhood, B., 2022. A systematic review of the therapeutic effects of resveratrol in combination with 5-fluorouracil during colorectal cancer treatment: with a special focus on the oxidant, apoptotic, and anti-inflammatory activities. Cancer Cell Int. 22 (1), 1–14. https://doi.org/10.1186/s12935-022-02561-7.

Nyström, L., Malmsten, M., 2018. Membrane interactions and cell selectivity of amphiphilic anticancer peptides. Curr. Opin. Colloid Interface Sci. 38, 1–17. https://doi.org/10.1016/j.cocis.2018.06.009.

Peredo-Lovillo, A., Hernández-Mendoza, A., Vallejo-Cordoba, B., Romero-Luna, H.E., 2022. Conventional and in silico approaches to select promising food-derived bioactive peptides: a review. Food Chem. X 13, 100183. https://doi.org/10.1016/j.fochx.2021.100183.

Phadke, G.G., Rathod, N.B., Ozogul, F., Elavarasan, K., Karthikeyan, M., Shin, K.-H., Kim, S.-K., 2021. Exploiting of secondary raw materials from fish processing industry as a source of bioactive peptide-rich protein hydrolysates. Mar. Drugs 19 (9), 480. https://doi.org/10.3390/md19090480.

Pi, D., Liu, Y., Shi, H., Li, S., Odle, J., Lin, X., Zhu, H., Chen, F., Hou, Y., Leng, W., 2014. Dietary supplementation of aspartate enhances intestinal integrity and energy status in weanling piglets after lipopolysaccharide challenge. J. Nutr. Biochem. 25 (4), 456–462. https://doi.org/10.1002/pro.4442.

Qiu, Y., You, J., Wang, K., Cao, Y., Hu, Y., Zhang, H., Fu, R., Sun, Y., Chen, H., Yuan, L., 2020. Effect of whole-course nutrition management on patients with esophageal cancer undergoing concurrent chemoradiotherapy: a randomized control trial. Nutrition 69, 110558. https://doi.org/10.1016/j.nut.2019.110558.

Rodrigues, C.H., Garg, A., Keizer, D., Pires, D.E., Ascher, D.B., 2022. Csm-peptides: a computational approach to rapid identification of therapeutic peptides. Protein Sci. 31 (10), e4442 https://doi.org/10.1002/pro.4442.

Roudi, R., Syn, N.L., Roudbary, M., 2017. Antimicrobial peptides as biologic and immunotherapeutic agents against cancer: a comprehensive overview. Front. Immunol. 8, 1320. https://doi.org/10.3389/fimmu.2017.01320.

Schaduangrat, N., Nantasenamat, C., Prachayasittikul, V., Shoombuatong, W., 2019. Acpred: a computational tool for the prediction and analysis of anticancer peptides. Molecules 24 (10), 1973. https://doi.org/10.3390/molecules24101973.

Sharma, A., Gupta, P., Kumar, R., Bhardwaj, A., 2016. Dpabbs: a novel in silico approach for predicting and designing anti-biofilm peptides. Sci. Rep. 6 (1), 21839 https://doi.org/10.3390/molecules24101973.

Shoombuatong, W., Schaduangrat, N., Nantasenamat, C., 2018. Unraveling the bioactivity of anticancer peptides as deduced from machine learning. EXCLI J. 17, 734. https://doi.org/10.17179/excli2018-1447.

Sinthusamran, S., Idowu, A.T., Benjakul, S., Prodpran, T., Yesilsu, A.F., Kishimura, H., 2020. Effect of proteases and alcohols used for debittering on characteristics and antioxidative activity of protein hydrolysate from salmon frames. J. Food Sci. Technol. 57, 473–483. https://doi.org/10.1007/s13197-019-04075-z.

Sougiannis, A., VanderVeen, B., Enos, R., Velazquez, K., Bader, J., Carson, M., Chatzistamou, I., Walla, M., Pena, M., Kubinak, J., 2019. Impact of 5 fluorouracil chemotherapy on gut inflammation, functional parameters, and gut microbiota. Brain Behav. Immun. 80, 44–55. https://doi.org/10.1016/j.bbi.2019.02.020.

Sridhar, K., Inbaraj, B.S., Chen, B.-H., 2021. Recent developments on production, purification and biological activity of marine peptides. Food Res. Int. 147, 110468 https://doi.org/10.1016/j.foodres.2021.110468.

Suo, S.-K., Zheng, S.-L., Chi, C.-F., Luo, H.-Y., Wang, B., 2022. Novel angiotensin-converting enzyme inhibitory peptides from tuna byproducts—milts: preparation, characterization, molecular docking study, and antioxidant function on h2o2-damaged human umbilical vein endothelial cells. Front. Nutr. 9 https://doi.org/10.3389/fnut.2022.957778.

Taieb, J., Tabernero, J., Mini, E., Subtil, F., Folprecht, G., Van Laethem, J.-L., Thaler, J., Bridgewater, J., Petersen, L.N., Blons, H., 2014. Oxaliplatin, fluorouracil, and leucovorin with or without cetuximab in patients with resected stage iii colon cancer (petacc-8): an open-label, randomised phase 3 trial. Lancet Oncol. 15 (8), 862–873. https://doi.org/10.1016/s1470-2045(14)70227-x.

Tohyama, N., Tanaka, S., Onda, K., Sugiyama, K., Hirano, T., 2013. Influence of anticancer agents on cell survival, proliferation, and CD4+ CD25+ Foxp3+ regulatory T cell-frequency in human peripheral-blood mononuclear cells activated by T cell-mitogen. Int. Immunopharm. 15 (1), 160–166. https://doi.org/10.1016/j.intimp.2012.11.008.

Vargas Casanova, Y., Rodríguez Guerra, J.A., Umaña Pérez, Y.A., Leal Castro, A.L., Almanzar Reina, G., Garcia Castaneda, J.E., Rivera Monroy, Z.J., 2017. Antibacterial synthetic peptides derived from bovine lactoferricin exhibit cytotoxic effect against mda-mb-468 and mda-mb-231 breast cancer cell lines. Molecules 22 (10), 1641. https://doi.org/10.3390/molecules22101641.

Wan, P., Chen, D., Chen, H., Zhu, X., Chen, X., Sun, H., Pan, J., Cai, B., 2020. Hypolipidemic effects of protein hydrolysates from trachinotus ovatus and identification of peptides implied in bile acid-binding activity using lc-esi-q-tof-ms/ms. RSC Adv. 10 (34), 20098–20109. https://doi.org/10.3390/molecules22101641.

Wang, G., Vaisman, I.I., van Hoek, M.L., 2022. Machine learning prediction of antimicrobial peptides. In: Computational Peptide Science: Methods and Protocols. Springer, pp. 1–37. https://doi.org/10.1007/978-1-0716-1855-4_1.

Wang, G., Xie, B., Su, Y., Gu, Q., Hao, D., Liu, H., Wang, C., Hu, Y., Zhang, M., 2021. Expression analysis of tissue factor pathway inhibitors tfpi-1 and tfpi-2 in paralichthys olivaceus and antibacterial and anticancer activity of derived peptides. Vet. Res. 52 (1), 1–13. https://doi.org/10.1186/s13567-021-00908-y.

Wang, P.-Y., Shuang, F.-F., Yang, J.-X., Jv, Y.-X., Hu, R.-Z., Chen, T., Yao, X.-H., Zhao, W.-G., Liu, L., Zhang, D.-Y., 2022. A rapid and efficient method of microwave-assisted extraction and hydrolysis and automatic amino acid analyzer determination of 17 amino acids from mulberry leaves. Ind. Crop. Prod. 186, 115271 https://doi.org/10.1016/j.indcrop.2022.115271.

Xiang, X.-W., Zhou, X.-L., Wang, R., Shu, C.-H., Zhou, Y.-F., Ying, X.-G., Zheng, B., 2021. Protective effect of tuna bioactive peptide on dextran sulfate sodium-induced colitis in mice. Mar. Drugs 19 (3), 127. https://doi.org/10.3390/md19030127.

Yaghoubzadeh, Z., Peyravii Ghadikolaii, F., Kaboosi, H., Safari, R., Fattahi, E., 2020. Antioxidant activity and anticancer effect of bioactive peptides from rainbow trout

(*oncorhynchus mykiss*) skin hydrolysate. Int. J. Pept. Res. Therapeut. 26 (1), 625–632. https://doi.org/10.1007/s10989-019-09869-5.

Yuan, E., Nie, S., Qi, C., Chang, B., Ren, J., 2021. Effect of scomberomorus niphonius peptide on the characteristics of resveratrol. Food Funct. 12 (22), 11449–11459. https://doi.org/10.1039/D1FO01333E.

Zhao, G.-X., Yang, X.-R., Wang, Y.-M., Zhao, Y.-Q., Chi, C.-F., Wang, B., 2019. Antioxidant peptides from the protein hydrolysate of Spanish mackerel (scomberomorous niphonius) muscle by in vitro gastrointestinal digestion and their in vitro activities. Mar. Drugs 17 (9), 531. https://doi.org/10.3390/md17090531.